



## A Single Crystal Study of CPO-27 and UTSA-74 for Nitric Oxide Storage and Release

Received 00th January 20xx,  
Accepted 00th January 20xx

Susan E. Henkelis,<sup>a</sup> Simon M. Vornholt,<sup>a</sup> David B. Cordes,<sup>a</sup> Alexandra M. Z. Slawin,<sup>a</sup> Paul S. Wheatley<sup>a</sup> and Russell E. Morris<sup>a,b\*</sup>

DOI: 10.1039/x0xx00000x

[www.rsc.org/](http://www.rsc.org/)

**Single crystal CPO-27-Mg, -Zn and its structural isomer UTSA-74 have been prepared through use of acid modulators; salicylic acid and benzoic acid, respectively. Salicylic acid directed the synthesis of CPO-27-Mg/Zn whereas benzoic acid the synthesis of UTSA-74. Through “in-house” SCXRD, DMF was seen to bind to the Zn<sup>2+</sup> and water to the Mg<sup>2+</sup> metal sites in CPO-27-M. Although the synthesis conditions were analogous for UTSA-74, DMF is too large to bind due to the proximity of the binding sites. A dissolution-recrystallisation transformation was examined from UTSA-74 to CPO-27-Zn. The release of nitric oxide was measured for each material.**

### Introduction

CPO-27-M (Coordination Polymer of Oslo; M = Co, Cu, Mg, Ni, Zn),<sup>1–5</sup> also termed MOF-74,<sup>6</sup> is one of the world’s most studied metal-organic frameworks (MOFs) due to the remarkably high density of coordinatively unsaturated metal sites (CUSs).<sup>7</sup> Now, typically produced under reflux conditions in a ratio of 1:2:4:304 for linker:salt:base:solvent, where the linker is 2,5-dihydroxyterephthalic acid and base is 1 M NaOH, these MOFs can be produced in high yield as microcrystalline powders.<sup>8</sup> Due to their large internal surface area and high porosity, MOFs have proven to have applications in biomedicine,<sup>2,9–11</sup> catalysis,<sup>12</sup> gas adsorption and delivery,<sup>13–16</sup> and sensing.<sup>8</sup> One such biomedical application has shown that nitric oxide can be stored within the pores of CPO-27-M materials and then released upon exposure to moisture. Thus demonstrating that they can be of use in medical applications such as catheters and stents to release a controlled amount of vasodilating NO.<sup>4,13,17</sup> Single crystal X-ray analysis is of great interest in order to locate cation-anion bonding sites in the structure and monitor how

these change with different synthesis conditions. It is most useful to track certain gas sorption processes in detail.<sup>18,19</sup> Single crystal analysis has been elusive for many materials from this family of MOFs.<sup>18,19</sup> Three crystal structures produced through single crystal X-ray analysis are currently recorded in the Cambridge Structure Database (CSD), including CPO-27-Zn,<sup>6</sup> -Mg<sup>20</sup> and -Co<sup>21</sup>. CPO-27-Cu,<sup>22</sup> -Mn,<sup>22</sup> -Fe<sup>23</sup> and -Ni<sup>24</sup> have been structurally characterised by neutron (Cu and Mn) and X-ray (Fe and Ni) powder diffraction. Each of these materials are synthesised with either added liquid water not pertaining to the hydrated salt (CPO-27-Zn, -Co, -Mg, -Mn and -Ni) or base (CPO-27-Mg, and -Cu).

With the use of acid modulators in the reaction system, CPO-27-Mg, -Zn and its recently discovered analogue UTSA-74 have been prepared in high purity, with single crystals large enough to be measured on an in-house diffractometer. Each material was prepared under solvothermal conditions at 150 °C without the need for the necessary base or added liquid water, hence conclusively disputing these components as being essential for synthesis of the target compounds.<sup>8,25,26</sup> The MOFs were analysed by powder X-ray diffraction (PXRD), single crystal X-ray diffraction (SCXRD), and scanning electron microscopy (SEM). UTSA-74 is a recently discovered analogue of CPO-27-Zn and is of much interest due to its dual channel system.<sup>27,28</sup> As such, UTSA-74 underwent nitric oxide loading and its release profile compared against single crystals of CPO-27-Zn. (Table 1, Full synthesis in E.S.I.).

Table 1. Experimental conditions for the synthesis of each metal-organic framework. All reactions were carried out at 150 °C.

MOF	Media	Modulator
UTSA-74	DMF/Butanol	Benzoic Acid
CPO-27-Zn	DMF/Ethanol	Salicylic Acid
CPO-27-Mg	DMF/Ethanol	Salicylic Acid

<sup>a</sup> School of Chemistry, EastChem, University of St Andrews, North Haugh, St Andrews, Fife, KY16 9ST, United Kingdom

<sup>b</sup> Department of Physical and Macromolecular Chemistry, Faculty of Sciences, Charles University Hlavova 8, 128 43 Prague 2, Czech Republic

Electronic Supplementary Information (ESI) available: [details of any supplementary information available should be included here]. See DOI: 10.1039/x0xx00000x

## Experimental

CPO-27-Zn, -Mg samples large enough for “in-house” diffraction were collected at 173 K on a Rigaku MM-007HF High Brilliance RA generator/confocal optics taLAB P100 diffractometer [Cu K $\alpha$  radiation ( $\lambda = 1.54187 \text{ \AA}$ )]. UTSA-74 samples were collected at 93 K on a Rigaku FR-X Ultrahigh Brilliance Microfocus RA generator/confocal optics with XtaLAB P200 diffractometer [Mo K $\alpha$  radiation ( $\lambda = 0.71075 \text{ \AA}$ )]. The structure solution was obtained using SHELXT<sup>29</sup> and refined by full-matrix least-squares against  $F^2$  using SHELXL-2018-3<sup>30</sup> within the Olex2<sup>31</sup> suite. All full occupancy non-hydrogen atoms were refined with anisotropic thermal displacement parameters. Aromatic hydrogen atoms were included at their geometrically estimated positions. CCDC 1863524; 1863523; 1863522 contains the supplementary crystallographic data for this paper. The data can be obtained free of charge from The Cambridge Crystallographic Data Centre via [www.ccdc.cam.ac.uk/structures](http://www.ccdc.cam.ac.uk/structures).

A Sievers 280i Nitric Oxide Analyser (NOA) was used to determine the amount of NO released in each material. The NO-loaded MOFs were introduced to the NOA and exposed to moisture (relative humidity of 11%), in order to replace the NO bound to the material, with water molecules. The resultant gas expelled can then be recorded in ppm/ppb.

## Results and Discussion

Two acid modulators were employed, benzoic and salicylic acids. Upon changing the modulator from salicylic acid to benzoic acid, yellow-green-coloured crystals of the structural isomer, UTSA-74 were afforded. Each material was Soxhlet extracted for 5 days in the corresponding alcohol to remove any remaining modulator or DMF used in the synthesis from the pores. They were then analysed through powder XRD to ensure the sample was phase pure (Fig. 1). A clear shift in the PXRD to higher  $2\theta$  can be seen for UTSA-74, indicating a smaller d-spacing between the channel systems. The decreased angle around the Zn<sup>2+</sup> metal site giving a smaller pore volume throughout the material.

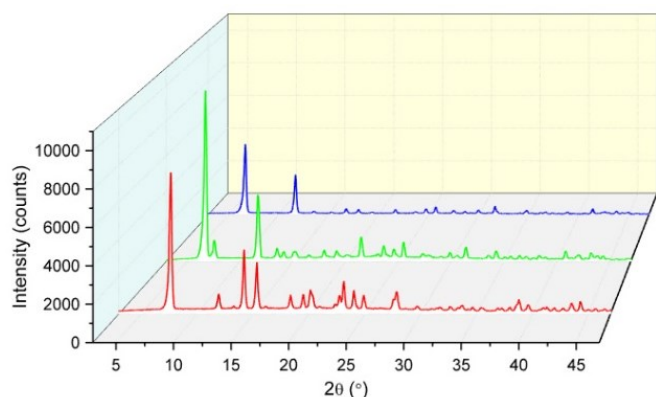


Figure 1. Powder X-ray diffraction patterns for CPO-27-Mg (blue), CPO-27-Zn (green) and UTSA-74 (red).

Secondly, after confirming that each material was phase pure through PXRD, single-crystal X-ray diffraction analysis was conducted on all three samples. Due to the synthesis conditions, DMF was present in the structure solution and seen to bind to the 2+ metal site with full occupancy for CPO-27-Zn (Figs. 2 and 3). For CPO-27-Mg however, the diffuse electron density was SQUEEZED out using the mask command in Olex2.<sup>32</sup> The two hydrated metal salts used contained different amounts of water (monohydrate and hexahydrate for Zn and

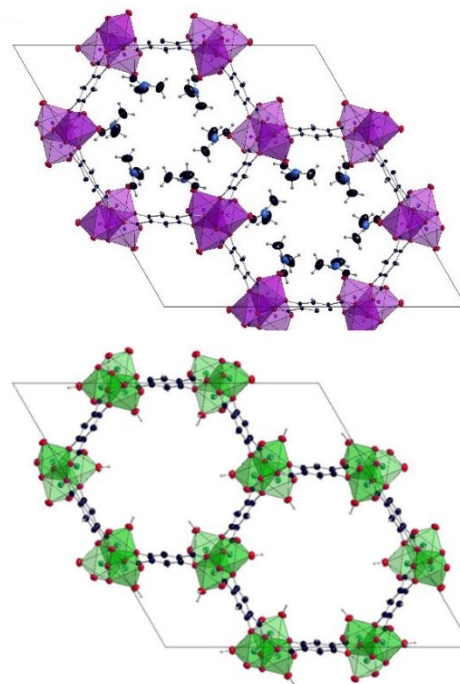


Figure 2. Structures of CPO-27-Zn with DMF molecules bound to the Zn<sup>2+</sup> site (TOP), and CPO-27-Mg showing water molecules bound to the Mg<sup>2+</sup> site (BOTTOM). Zn SBU – purple; Mg SBU – green. As viewed down the a-axis.

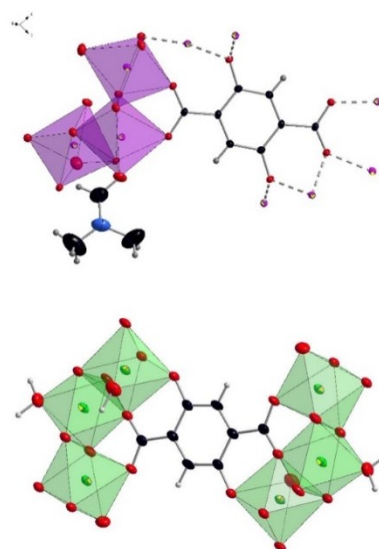


Figure 3. The chains of CPO-27-Zn (TOP) and CPO-27-Mg (BOTTOM) highlighting both the 2,5-dihydroxyterephthalic acid linker and attached DMF molecule to the Zn<sup>2+</sup> metal site and coordinated water to the Mg<sup>2+</sup> site. Viewed down the b-axis.

Mg respectively) and as such changed the amount of water present in the reacting mixture. Oxo-phyllic  $Mg^{2+}$  is a hard metal and as such it prefers to ionically bind through its co-ordinately unsaturated sites, and therefore we see water bind to these CUSs.  $Zn^{2+}$  is an intermediate acid (neither soft nor hard), so prefers to bind covalently. In CPO-27-Zn, DMF is seen to preferentially bind through covalent bonds. However, when we change the modulator to form UTSA-74, the pore size is too small to accommodate covalent bonding to DMF, and as such we see water ionically bind.

Both CPO-27 materials are hereby presented in space group  $R\bar{3}$ . The structural isomer, UTSA-74, exhibited the zinc structural building unit (SBU) in both tetrahedral and octahedral coordination, thus giving rise to a large and small pore channel system (Fig. 4).<sup>27</sup>

UTSA-74 was prepared in conditions analogous to the CPO-27 materials. However, the proximity of the binding sites (4 Å) are too close to accommodate binding to DMF and as such DMF is not seen in the refinement. Each octahedral  $Zn^{2+}$  site has one axial bound water molecule pointing into the pore and one pointing out. Original literature presented the structure in space group  $R\bar{3}c$ ;<sup>27,28</sup> however this was only seen when disorder was removed from the structure. We hereby present the space group as  $R3c$ , with all disorder in the structure accounted for.

Due to a smaller pore size than CPO-27, when coordinated water is present, the pores are completely blocked (Fig. 4). Upon activation at 200 °C under dynamic vacuum ( $2 \times 10^{-4}$  mbar), the two axial water molecules can be selectively removed, generating open  $Zn^{2+}$  metal sites which are able to bind two gas molecules per metal centre on the pore surfaces of the 1-dimensional channels.

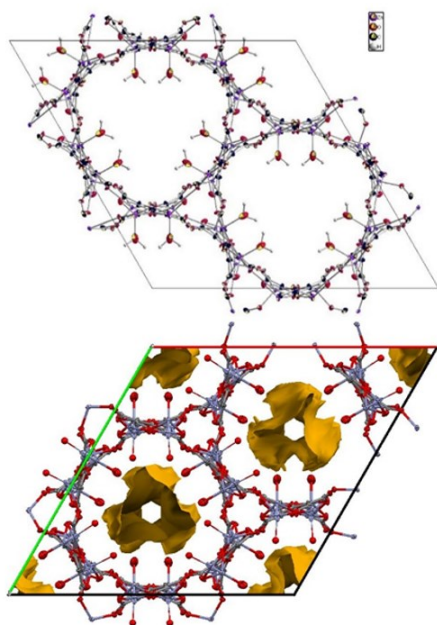


Figure 4. Structures of UTSA-74 showing  $Zn^{2+}$  in both tetrahedral and octahedral coordination, giving rise to a small and large pore channel system. Each octahedral  $Zn^{2+}$  has 1 axial bound water molecule pointing into the pore and 1 pointing out (TOP). Void space with solvent molecules bound, showing the pores are blocked (BOTTOM). Viewed along the c-axis

Each MOF was further analysed by scanning electron microscopy (SEM). Unlike the CPO-27 materials which presented a needle-like morphology, UTSA-74 afforded a morphology of large hexagonal rods (Fig. 5).

Upon submerging the UTSA-74 crystals in water at room temperature, what, at first glance, looks to be a rapid single crystal – single crystal transformation is proceeding due to hydrolysis. This phenomenon has been first presented as an *in situ* study by Bueken *et al.*<sup>28</sup> Here we examine this hydrolysis through SEM and SCXRD. As shown in Figure 6, the UTSA-74 rods are slowly being “eaten away” and the newly formed CPO-27-Zn needles growing on the surface. From the SEM, it is now apparent that a simple single crystal – single crystal transformation is not occurring. The mechanism appears to be in two steps. First a dissolution of the UTSA-74 into the water and then the formation of CPO-27-Zn on the surface of the remaining UTSA-74 crystals. As the newly formed crystals of CPO-27-Zn are not formed in solution, it seems that UTSA-74 is being used as a scaffold. After 3 hr, the UTSA-74 has been fully consumed and CPO-27-Zn is the sole material present. After full hydrolysis, the crystals of CPO-27-Zn are too small to diffract sufficiently for structural determination using an in-house instrument; however a unit cell check confirmed that the structural transformation to CPO-27-Zn had taken place.

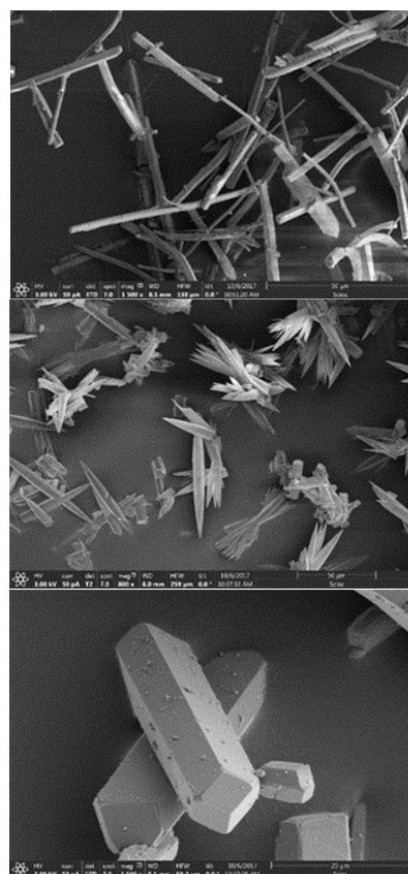


Figure 5. SEM images of CPO-27-Mg, 50  $\mu m$  (TOP); CPO-27-Zn, 50  $\mu m$  (MIDDLE); UTSA-74, 20  $\mu m$  (BOTTOM). Highlighting a needle morphology for the CPO-27 family and a rod formation for UTSA-74.

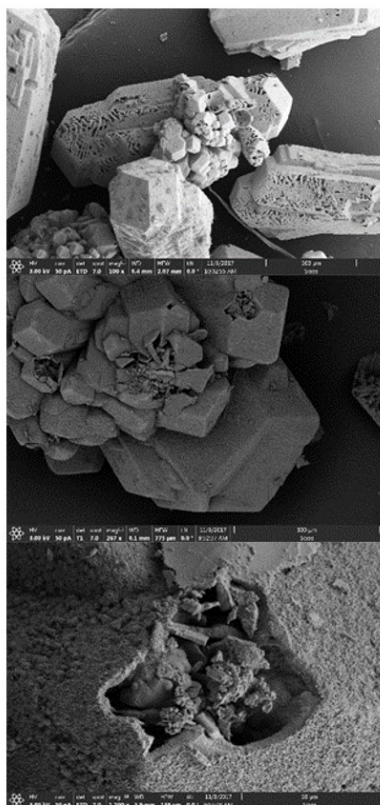


Figure 6. The single crystal - single crystal transformation of UTSA-74 to CPO-27-Zn by hydrolysis as shown by SEM images at a scale of 500  $\mu\text{m}$  (TOP), 300  $\mu\text{m}$  (MIDDLE) and 100  $\mu\text{m}$  (BOTTOM). The rods of UTSA-74 look to be being eaten away and the new CPO-27-Zn needles growing on the surface. This has also been recorded by single crystal X-ray diffraction, however due to the size of the newly transformed CPO-27-Zn, only a unit cell match could be performed.<sup>28</sup>

Both CPO-27-Zn and UTSA-74 were activated at 200 °C under dynamic vacuum to remove coordinated solvent molecules. The dehydrated materials were then subjected to nitric oxide gas, an immediate colour change, significantly intensifying the green colour, could be seen indicating that the gas had been adsorbed onto the CUSs. Loaded materials were then exposed to three consecutive vacuum/argon cycles to remove excessive physisorbed nitric oxide prior to analysis of nitric oxide release. CPO-27-Zn releases slightly more than UTSA-74 with 0.088 and 0.067 mmol, respectively (Fig. 7).

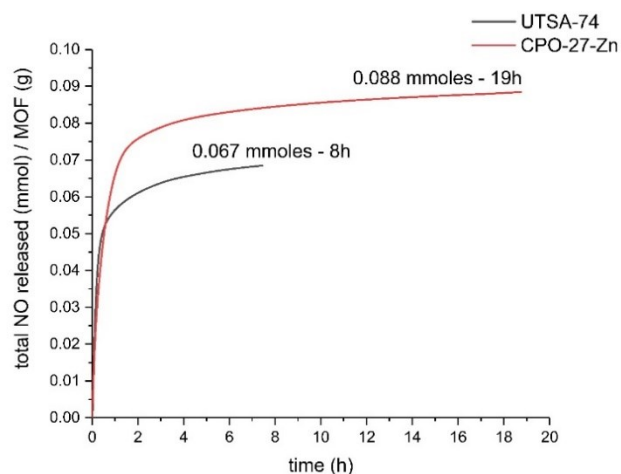


Figure 7. Nitric oxide release profiles for UTSA-74 (black) and CPO-27-Zn (red)

## Conclusions

Single crystal CPO-27-Mg, -Zn and its structural isomer UTSA-74 have been prepared through use of two acid modulators, salicylic acid and benzoic acid, respectively. These MOFs were analysed by single crystal X-ray diffraction and scanning electron microscopy (SEM). Crystals large enough for “in-house” SCXRD were collected, where DMF was seen to bind to the 2+ metal sites in CPO-27-Zn, however although the synthesis conditions were analogous for UTSA-74, DMF is too large to bind due to the proximity of the binding sites (4 Å). The CPO-27 materials were afforded in a needle-like morphology, whilst the UTSA-74 produced larger rods. The dissolution-recrystallisation of UTSA-74 into CPO-27-Zn transformation via hydrolysis was examined by SEM and a unit cell match confirmed. The uptake and release of nitric oxide was measured for each zinc-containing material.

## Conflicts of interest

There are no conflicts to declare.

## Acknowledgements

The authors would like to thank: The EPSRC (grants: EP/K005499/1; EP/K503162/1) for funding opportunities and the EPSRC Capital for Great Technologies (EP/L017008/1).

## Notes and references

- 1 M. J. Katz, A. J. Howarth, P. Z. Moghadam, J. B. DeCoste, R. Q. Snurr, J. T. Hupp and O. K. Farha, *Dalt. Trans.*, 2016, **45**, 4150–4153.
- 2 A. C. McKinlay, P. K. Allan, C. L. Renouf, M. J. Duncan, P. S. Wheatley, S. J. Warrender, D. Dawson, S. E. Ashbrook, B. Gil, B. Marszalek, T. Düren, J. J. Williams, C. Charrier, D. K. Mercer, S. J. Teat and R. E. Morris, *APL Mater.*, 2014, **2**,

- 124108.
- 3 F. Bonino, S. Chavan, J. G. Vitillo, E. Groppo, G. Agostini, C. Lamberti, P. D. C. Dietzel, C. Prestipino and S. Bordiga, *Chem. Mater.*, 2008, **20**, 4957–4968.
- 4 D. Cattaneo, S. J. Warrender, M. J. Duncan, C. J. Kelsall, M. K. Doherty, P. D. Whitfield, I. L. Megson and R. E. Morris, *RSC Adv.*, 2016, **6**, 14059–14067.
- 5 S. M. Vornholt, S. E. Henkelis and R. E. Morris, *Dalt. Trans.*, 2017, **46**, 8298–8303.
- 6 N. L. Rosi, J. Kim, M. Eddaoudi, B. Chen, M. O’Keeffe and O. M. Yaghi, *J. Am. Chem. Soc.*, 2005, **127**, 1504–18.
- 7 I. Senkovska, K. A. Cychosz, P. Llewellyn, M. Thommes and S. Kaskel, in *The Chemistry of Metal-Organic Frameworks: Synthesis, Characterization, and Applications*, ed. S. Kaskel, Wiley-VCH Verlag GmbH & Co. KGaA, Weinheim, Germany, 2016, pp. 575–605.
- 8 L. Garzón-Tovar, A. Carné-Sánchez, C. Carbonell, I. Imaz and D. MasPOCH, *J. Mater. Chem. A*, 2015, **3**, 20819–20826.
- 9 P. K. Allan, P. S. Wheatley, D. Aldous, M. I. Mohideen, C. Tang, J. A. Hriljac, I. L. Megson, K. W. Chapman, G. De Weireld, S. Vaesen and R. E. Morris, *Dalton Trans.*, 2012, **41**, 4060–6.
- 10 N. J. Hinks, A. C. McKinlay, B. Xiao, P. S. Wheatley and R. E. Morris, *Microporous Mesoporous Mater.*, 2010, **129**, 330–334.
- 11 S. R. Miller, E. Alvarez, L. Fradcourt, T. Devic, S. Wuttke, P. S. Wheatley, N. Steunou, C. Bonhomme, C. Gervais, D. Laurencin, R. E. Morris, A. Vimont, M. Daturi, P. Horcajada and C. Serre, *Chem. Commun. (Camb.)*, 2013, **49**, 7773–5.
- 12 D. Ruano, M. Díaz-García, A. Alfayate and M. Sánchez-Sánchez, *ChemCatChem*, 2015, **7**, 674–681.
- 13 D. Cattaneo, S. J. Warrender, M. J. Duncan, R. Castledine, N. Parkinson, I. Haley and R. E. Morris, *Dalton Trans.*, 2015, **45**, 618–629.
- 14 S. Chavan, F. Bonino, L. Valenzano, B. Civalieri, C. Lamberti, N. Acerbi, J. H. Cavka, M. Leistner and S. Bordiga, *J. Phys. Chem. C*, 2013, **117**, 15615–15622.
- 15 S. Chavan, J. G. Vitillo, E. Groppo, F. Bonino, C. Lamberti, P. D. C. Dietzel and S. Bordiga, *J. Phys. Chem. C*, 2009, **113**, 3292–3299.
- 16 P. D. C. Dietzel, B. Panella, M. Hirscher, R. Blom and H. Fjellvåg, *Chem. Commun.*, 2006, 959.
- 17 A. C. McKinlay, B. Xiao, D. S. Wragg, P. S. Wheatley, I. L. Megson and R. E. Morris, *J. Am. Chem. Soc.*, 2008, **130**, 10440–10444.
- 18 P. D. C. Dietzel, P. A. Georgiev, J. Eckert, R. Blom, T. Strässle and T. Unruh, *Chem. Commun.*, 2010, **46**, 4962.
- 19 A. C. Mckinlay, B. Xiao, D. S. Wragg, P. S. Wheatley, I. L. Megson and R. E. Morris, *J. Am. Chem. Soc.*, 2008, **130**, 10440–10444.
- 20 P. D. C. Dietzel, R. Blom and H. Fjellvåg, *Eur. J. Inorg. Chem.*, 2008, **2008**, 3624–3632.
- 21 M. I. Gonzalez, J. A. Mason, E. D. Bloch, S. J. Teat, K. J. Gagnon, G. Y. Morrison, W. L. Queen and J. R. Long, *Chem. Sci.*, 2017, **8**, 4387–4398.
- 22 M. H. Rosnes, M. Opitz, M. Frontzek, W. Lohstroh, J. P. Embs, P. A. Georgiev and P. D. C. Dietzel, *J. Mater. Chem. A*, 2015, **3**, 4827–4839.
- 23 M. Märzc, R. E. Johnsen, P. D. C. Dietzel and H. Fjellvåg, *Microporous Mesoporous Mater.*, 2012, **157**, 62–74.
- 24 F. Bonino, S. Chavan, J. G. Vitillo, E. Groppo, G. Agostini, C. Lamberti, P. D. C. Dietzel, C. Prestipino and S. Bordiga, *Local Structure of CPO-27-Ni Metallorganic Framework upon Dehydration and Coordination of NO*, .
- 25 N. E. Ghermani, G. Morgant, J. d’Angelo, D. Desmaële, B. Fraisse, F. Bonhomme, E. Dichi and M. Sgahier, *Polyhedron*, 2007, **26**, 2880–2884.
- 26 S. E. Henkelis, L. J. McCormick, D. B. Cordes, A. M. Z. Slawin and R. E. Morris, *Inorg. Chem. Commun.*, 2016, **65**, 21–23.
- 27 F. Luo, C. Yan, L. Dang, R. Krishna, W. Zhou, H. Wu, X. Dong, Y. Han, T.-L. Hu, M. O’Keeffe, L. Wang, M. Luo, R.-B. Lin and B. Chen, *J. Am. Chem. Soc.*, 2016, **138**, 5678–5684.
- 28 B. Bueken, H. Reinsch, N. Heidenreich, A. Vandekerckhove, F. Vermoortele, C. E. A. Kirschhock, N. Stock, D. De Vos and R. Ameloot, *CrystEngComm*, 2017, **19**, 4152–4156.
- 29 G. M. Shelbrick, *Acta Crystallogr. Sect. A Found. Crystallogr.*, 2008, **64**, 112–122.
- 30 G. M. Shelbrick, *Acta Crystallogr. Sect. C Struct. Chem.*, 2015, **71**, 3–8.
- 31 O. V. Dolomanov, L. J. Bourhis, R. J. Gildea, J. A. K. Howard and H. Puschmann, *J. Appl. Crystallogr.*, 2009, **42**, 339–341.
- 32 A. L. Spek and IUCr, *Acta Crystallogr. Sect. C Struct. Chem.*, 2015, **71**, 9–18.